BULLETIN OF THE POLISH ACADEMY OF SCIENCES
TECHNICAL SCIENCES, Vol. 68, No. 2, 2020
DOI: 10.24425/bpasts.2020.133108

Edge termination design for 1.7 kV silicon carbide p-i-n diodes

A. TAUBE[1,2]* and M. SOCHACKI[1]

[1] Warsaw University of Technology, Institute of Microelectronics and Optoelectronics, ul. Koszykowa 75, 00-662 Warsaw, Poland
[2] Łukasiewicz Research Network – Institute of Electron Technology, al. Lotników 32/46, 02-668 Warsaw, Poland

Abstract. In this work, in order to obtain breakdown voltage values of the 4H-SiC p-i-n diodes above 1.7kV, three designs have been examined: single-zone junction termination extention (JTE), double-zone JTE and a structure with concentric rings outside each of the areas of the double-zone JTE (space-modulated JTE). The influence of geometry and the level of p-type doping in the JTE area as well as the charge at the interface between the p-type JTE area and the passivation layer on the diode breakdown voltage was studied. The effect of statistical dispersion of drift layer parameters (thickness, doping level) on diodes breakdown voltage with various JTE structures was investigated as well. The obtained results showed that the breakdown volatge values for a diode with single zone JTE are very sensitive both to the dose of JTE area and charge accumulated at the JTE/dielectric interface. The use of a double zone or space-modulated JTE structures allows for obtaining breakdown voltage above 1.7 kV for a much wider range of doping parameters and with better tolerance to positive charge at the JTE/dielectric interface, as well as better tolerance to statistical dispersion of active layer parameters compared to a single zone JTE structure.

Key words: edge termination, silicon carbide, 4H-SiC, p-i-n diode, breakdown voltage, JTE.

1. Introduction

Semiconductor diodes are the basic components of power factor correction (PFC) systems used in power electronics, which create a huge market for silicon carbide power devices [1]. PFC systems must be resistant to short-circuit conditions, which increase the requirements for surge-current capabilities of semiconductor devices. High values of surge-currents carried by semiconductor diodes appear in PFC systems also when the device is switched on and are also generated by highly distorted voltage and current waveforms [2]. The PFC system must react to surge-currents with time constants at the level of a few milliseconds. A desirable feature of the used semiconductor diodes is therefore an increased conductivity under surge-current conditions. This requirement is mainly fulfilled by p-i-n junction diodes, which in the case of a surge-current are characterized by a lower voltage drop and, as a result, by lower power losses converted into dissipated heat as compared to the Schottky diodes [1, 3]. The protection of this type of circuits with junction diodes definitely increases the safety and reliability of the PFC system. The basic market for the junction diodes are applications requiring very low leakage currents with high reverse bias and low thermal resistance, which is basically not achievable for Schottky diodes [3], and all kinds of protection circuits, where components are exposed to surge-currents with a long duration at the level above 10 ms. The use of junction diodes allows for eliminating many elements responsible for shortening the duration of the surge current (inrush current) from the PFC system design and mitigation of current waveforms when switching to short circuit conditions.

In addition to issues related to the development of high-quality 4H-SiC epitaxial layers with low defect density, such as micropipes, stacking faults, carbon vacancies [4], one of the most important issues related to the development of high-voltage silicon carbide junction diodes is the appropriate design of the edge termination [5]. Properly designed edge termination allows to obtain uniform distribution of the electric field near the p-n junction at high reverse voltages, leading to increased values of the breakdown voltage, close to the theoretically ideal ones resulting from the electrophysical properties of silicon carbide. One of the techniques used for edge termination is JTE (junction termination extension), which is formed by a p-type region located around the outer edge of the anode [6, 7].

In this work, we performed simulations of several JTE designs for 1.7 kV 4H-SiC p-i-n diodes. The influence of geometry and the level of p-type doping in the JTE region as well as the charge at the interface between the p-type JTE area and the passivation layer on the diode breakdown voltage was studied. Moreover, in contrast to other works, the effect of statistical dispersion of drift layer parameters (thickness, doping level) on diodes breakdown voltage with various JTE structures was investigated as well.

2. Device structure and simulation details

Schematic cross-sections through the simulated structures of mesa-type [8] 4H-SiC p-i-n diodes with various JTE structures are shown in Fig. 1. The thickness and doping of drift layer grown on highly doped n^+ substrate ($N_D = 5\times10^{18}$ cm^{-3}) t_{epi} = 13 μm and $N_{D,epi} = 7.2\times10^{15}$ cm^{-3} were chosen to

---

*e-mail: ataube@ite.waw.pl

Manuscript submitted 2019-07-16, revised 2019-12-12, initially accepted for publication 2020-01-20, published in April 2020

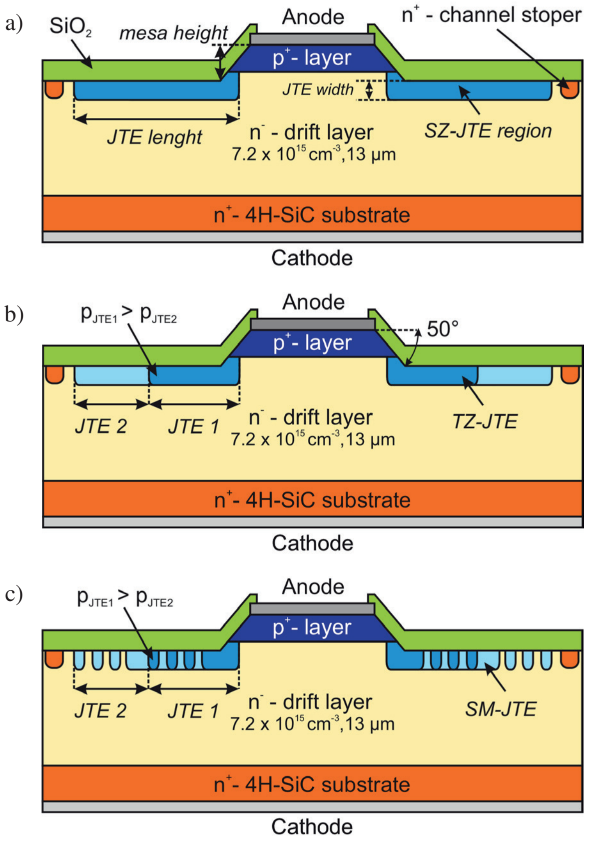

Fig. 1. Structure of simulated 4H-SiC p-i-n diode with a) single zone JTE (SZ-JTE); b) two-zone JTE (TZ-JTE) and c) space-modulated JTE (SM-JTE) edge terminations

obtain ideal breakdown voltage around 2100–2300 V [9]. The p-type anode consisted of 1 μm p$^+$ epilayer (N$_A$ = 1×10^{19} cm^{-3}) and 0.5 μm p^{++} subcontact layer doped to N$_A$ = 5×10^{19} cm^{-3}. The mesa height and angle was chose to be 2 μm and 50°, respectively. It was assumed that the surface of the diode is passivated with a 500 nm thick layer of SiO$_2$ (relative permittivity $\varepsilon_r = 3.9$). For anode and cathode, an ideal ohmic contact was assumed. In order to obtain breakdown voltage of the diode above 1.7 kV three different JTE designs have been selected: single-zone JTE (SZ-JTE) in the form of p-type ring outside the mesa-type structure (Fig. 1a) [7, 10, 11], two-zone JTE (TZ-JTE) in the form of two p-type rings outside the mesa-type structure differing in the dose and length (Fig. 1b) [10, 11] and finally with the space-modulated JTE structure (SM-JTE) with concentric rings outside each of the areas of the double-zone JTE structure (Fig. 1c) [11–13]. The JTE region is electrically connected to the anode as it slightly overlaps the p$^+$ layer at the mesa edge. In the case of double-zone JTE structure as well as the space-modulated JTE structure, two photolithography and implantation/annealing processes are needed for their fabrication. One aims to define the outer area of JTE with a smaller dose p$_{JTE2}$ (over the length L$_{JTE2}$), through the ion implantation on the total JTE length L$_{JTE}$, and the second one to fabricate the inner JTE region (for length L$_{JTE1}$) with higher dose (p$_{JTE1}$) at the edge of the mesa structure [10, 12]. The total dose in this case means the sum of the dose (doping level) of aluminum ion implantation into both the JTE1 and JTE2 areas. In the case of a single-zone JTE structure, the total JTE length L$_{JTE}$ varied from 5 μm to 60 μm. For all JTE structures, the depth of the JTE region W$_{JTE}$ area was 1 μm and was defined as the edge of the constant p-type dopant profile with gaussian tail with a maximum dose ranging from 4×10^{16} cm^{-3} to 2.8×10^{17} cm^{-3} (4×10^{17} cm^{-3} for SM-JTE). The diode structure also contained a highly doped n$^+$ – ring (channel stopper), which prevents current leakage on the surface [14].

The simulations were carried out using Silvaco ATLAS environment [15]. One of the most important 4H-SiC models used for breakdown voltage simulation is carrier generation through impact ionization process with impact ionization coefficients dependent on the electric field values. We choose an anisotropic impact ionization model with parameters values as proposed in [16, 17].

3. Results and discussion

3.1. Single-zone junction termination extension (SZ-JTE). Fig. 2a show the breakdown voltage of 4H-SiC p-i-n diode as a function of JTE dose (for JTE length 60 μm). The breakdown voltage increases linearly with JTE dose reaching maximum of 2293 V for a p$_{JTE}$ = 1.11×10^{17} cm^{-3}. For a dose slightly higher than the optimal one, an abrupt drop in the breakdown voltage to the values below 1700 V can be observed, with saturation at about 770 V for the highest doses. The JTE dose range, for which the breakdown voltage was over 1700 V, ranged from 8×10^{16} cm^{-3} to 1.13×10^{17} cm^{-3}.

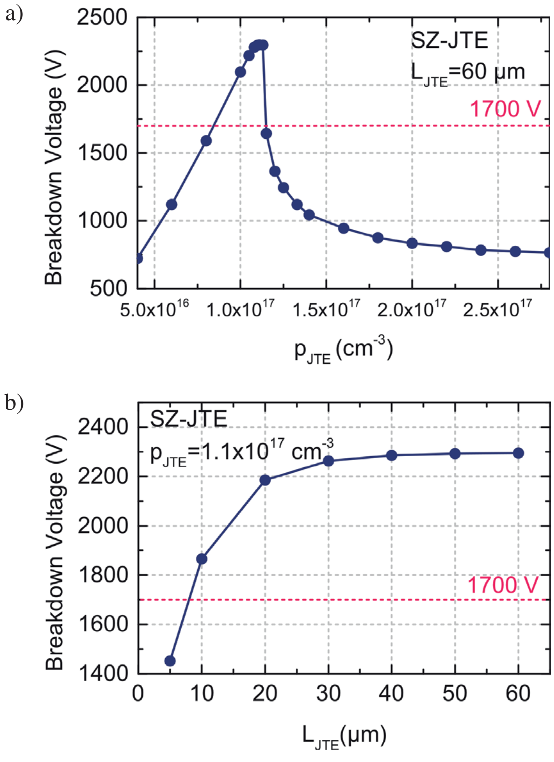

Fig. 2. Breakdown voltage of 4H-SiC p-i-n diode with SZ-JTE as a function of: a) JTE dose; b) JTE length

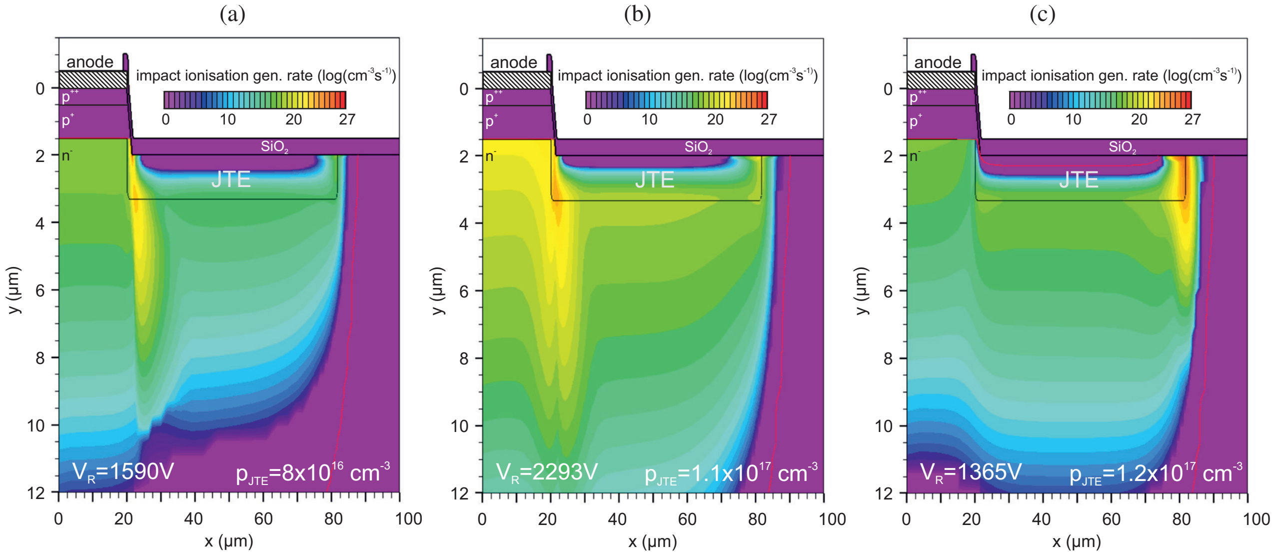

Fig. 3. Distribution of impact ionization generation rate at the breakdown for 4H-SiC p-i-n diode with SZ-JTE for JTE dose: a) 8×10^{16} cm^{-3}; b) 1.1×10^{17} cm^{-3}; c) 1.2×10^{17} cm^{-3}

In order to explain the observed dependence of the breakdown voltage on the JTE dose, in Fig. 3 the impact ionization generation rate at the breakdown for 4H-SiC p-i-n diode with SZ-JTE for a dose of 8×10^{16} cm^{-3}, 1.1×10^{17} cm^{-3}, 1.2×10^{17} cm^{-3} was shown (i.e. for a dose where the breakdown voltage does not reach the maximum value, for a dose close to the optimum one and for a dose above the optimum value). For a dose smaller than the optimal one, the breakdown occurs at the edge of the mesa structure, where the value of impact ionization generation rate is the highest. For an optimal dose, we can observe a more even distribution of the impact ionization generation rate at the p-n junction of the diode, with the maximum located at the inner edge of the JTE region. Whereas, the JTE dose greater than optimal one causes the shift of the maximum of impact ionization generation rate, and thus the peak of the electric field, to the outer edge of the JTE region and cause uniform distribution of the impact ionization generation rate near the p-n junction of the diode.

Simulations were also carried out to investigate the effect of the JTE length (L_{JTE}) on the breakdown voltage. The dependence of the breakdown voltage on the length of the JTE region for the dose 1.1×10^{17} cm^{-3} is shown in Fig. 2b. The breakdown voltage increases as the L_{JTE} increases and becomes saturated for $L_{JTE} = 60$ µm which is more than four times longer than drift layer thickness. This value was chosen for further simulations.

An important effect affecting the distribution of the electric field at high reverse voltage, and thus the diode breakdown voltage, is the presence of an effective electric charge at the dielectric/semiconductor interface, in particular on the surface of the JTE region [18]. This charge generally comes from surface states at the dielectric/semiconductor interface or is located in the volume of the dielectric layer [19, 20]. The simulations of the diode breakdown voltage for a JTE dose varied from 4×10^{16} cm^{-3} to 2.8×10^{17} cm^{-3} and surface charge density (Q_{it}) at the interface between JTE region and SiO$_2$ layer ranging from $+1\times10^{11}$ cm^{-2} to $+1\times10^{13}$ cm^{-2} were carried out. Figure 4a shows the dependence of the breakdown voltage on the JTE dose for JTE length $L_{JTE} = 60$ µm and five different Q_{it} values in the range from $+1\times10^{12}$ cm^{-2} to $+5\times10^{12}$ cm^{-2}. The positive charge on the surface of the JTE

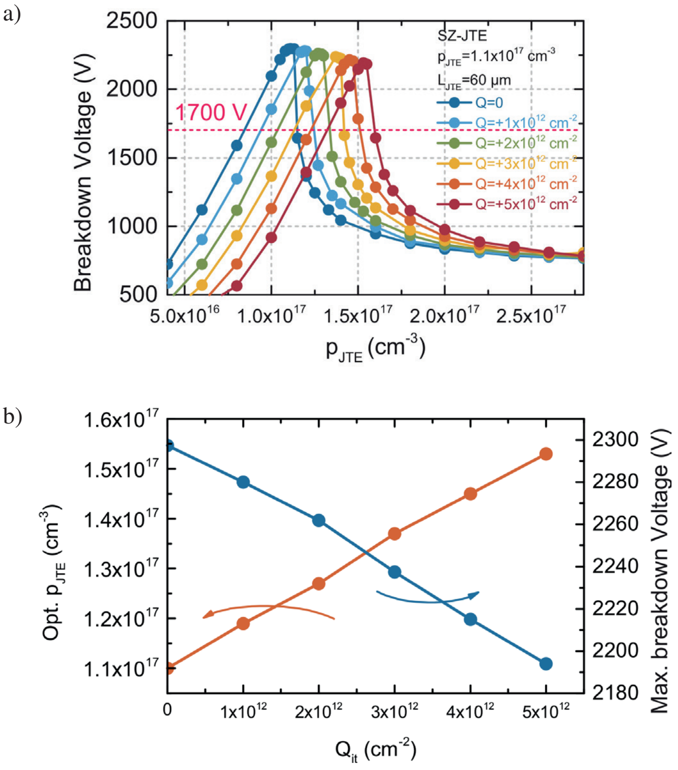

Fig. 4. a) Breakdown voltage of 4H-SiC p-i-n diode with SZ-JTE as a function of JTE dose for different Q_{it} values. b) The influence of Q_{it} values on the maximum breakdown voltage and optimal JTE dose

region shifts the breakdown voltage vs. JTE dose curve towards the larger values of the JTE dose. Basically, the shape of these curves stays unchanged. The value of the optimal dose increases with the increase of the surface charge, and this relation is almost linear (Fig. 4b). For $Q_{in} = +5\times10^{12}$ cm^{-2}, the optimal value of the dose is 1.53×10^{17} cm^{-3} compared to 1.11×10^{17} cm^{-3} for $Q_{it} = 0$. In contrast, the breakdown voltage value for the optimal dose decreases linearly with the increase of the Q_{it} charge from 2293 V for $Q_{it} = 0$ to 2200 V for $Q_{it} = +1\times10^{12}$ cm^{-2} (Fig. 4b). The effect of surface charge is particularly important for p-i-n diodes with a single JTE structure, because the relationship between breakdown voltage and dose is very steep.

To illustrate the effect of the Q_{it} charge on the breakdown voltage, the breakdown voltage values for $p_{JTE} = 1.1\times10^{17}$ cm^{-3} and Q_{it} from $+1\times10^{11}$ cm^{-2} to $+1\times10^{13}$ cm^{-2} were shown in the Fig. 5. Breakdown voltage decreases as Q_{it} charge value increases. This relationship is not linear in the whole Q_{it} range. An increase in the Q_{it} value from $+1\times10^{11}$ cm^{-2} to $+1\times10^{12}$ cm^{-2} results in the decrease of breakdown voltage from 2293 V to 2130 V, while the increase of the charge in the range from $+1\times10^{12}$ cm^{-2} to $+1\times10^{13}$ cm^{-2} results in the reduction of breakdown voltage from 2130 V to about 600 V. Real Q_{it} charge values range from $+1\times10^{11}$ cm^{-2} to even $+1\times10^{12}$ cm^{-2} [21], therefore when designing the edge termination, the occurrence of a non-zero Q_{it} value should be taken into account and the JTE region should be designed carefully to obtain the sensitivity of the breakdown voltage value on the surface charge density as low as possible.

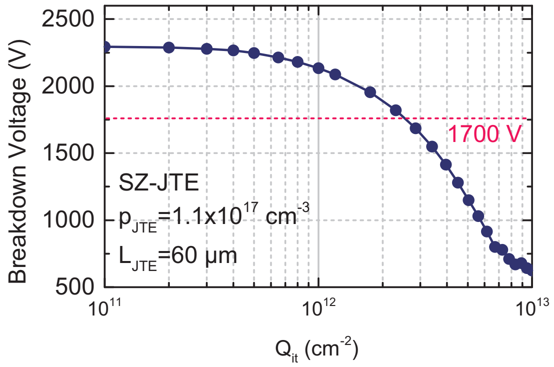

Fig. 5. The dependence of the breakdown voltage of 4H-SiC p-i-n diode with SZ-JTE for $p_{JTE} = 1.1\times10^{17}$ cm^{-3} as a function of Q_{it} values

3.2. Double-zone junction termination extension (TZ-JTE)

The idea of using the double-zone JTE structure assumes a spatial change in the JTE area applied to obtain a more even distribution of the electric field and to reduce the electric field value at the surface, and especially to increase the tolerance of the breakdown voltage to the JTE dose [7, 10]. In this work, at first the simulations of diodes with TZ-JTE were performed, for which the total JTE length was 60 μm and the dose ratio of the first and second JTE region $p_{JTE1} : p_{JTE2}$ was 1.5 : 1 for the ratio of L_{JTE1} to L_{JTE2} of 1 : 3, 1 : 1 and 3 : 1, respectively.

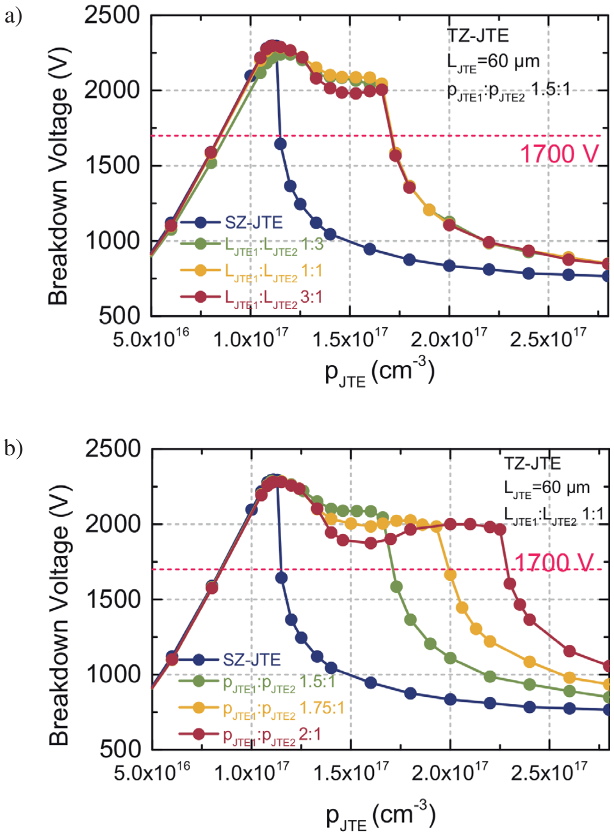

Fig. 6. Breakdown voltage of 4H-SiC p-i-n diode with TZ-JTE as a function of JTE dose for different: a) $L_{JTE1} : L_{JTE2}$ ratio for $p_{JTE1} : p_{JTE2} = 1.5 : 1$ and b) for different $p_{JTE1} : p_{JTE2}$ ratio for $L_{JTE1} : L_{JTE2} = 1 : 1$

Figure 6a shows the dependence of the breakdown voltage of 4H-SiC p-i-n diode with TZ-JTE as a function of JTE dose for different $L_{JTE1} : L_{JTE2}$ ratio. A similar relationship for a SZ-JTE structure is shown for comparison.

Similarly to a single-zone JTE structure (SZ-JTE), the breakdown voltage increases with the increase of the JTE area to a maximum of 2293 V for a dose of 1.11×10^{17} cm^{-3} regardless of the $L_{JTE1} : L_{JTE2}$ ratio. In comparison to SZ-JTE, in the case of TZ-JTE, the breakdown voltage drops slightly after exceeding the optimal value of the JTE dose, and a sharp drop in voltage can be observed for a dose equal to 1.66×10^{17} cm^{-3}. Changes in the case of different $L_{JTE1} : L_{JTE2}$ ratios are visible for the JTE dose range from 1.13×10^{17} cm^{-3} to 1.66×10^{17} cm^{-3}. In this range the diodes with TZ-JTE for the $L_{JTE1} : L_{JTE2}$ ratio equal to 1:1 are characterized by the highest breakdown voltages. However, impact of $L_{JTE1} : L_{JTE2}$ ratio within JTE dose range is relatively small. Figure 7 shows the distribution of impact ionization generation rate at the breakdown for 4H-SiC p-i-n diode with SZ-JTE and TZ-JTE for JTE dose of 1.2×10^{17} cm^{-3}. Distribution of carrier generation in the case of TZ-JTE is more uniform, especially in the area under contact of the anode and at the boundary of the JTE1 and JTE2 regions.

A significant change of the relationship between breakdown voltage and JTE dose was observed for various $p_{JTE1} : p_{JTE2}$

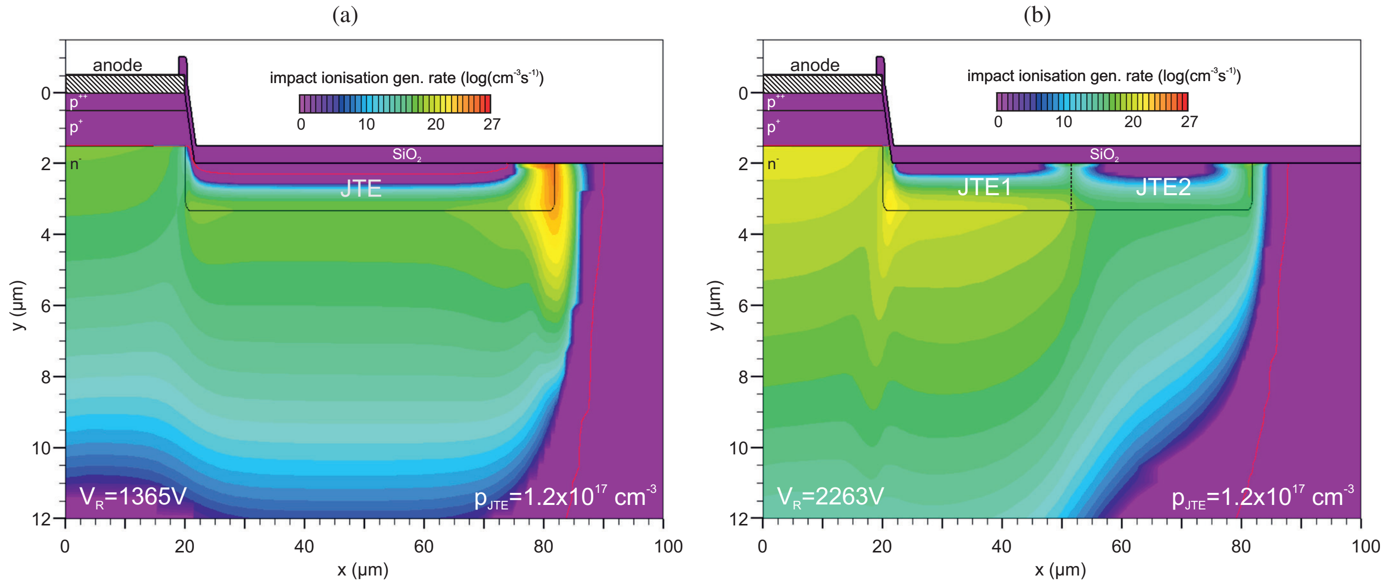

Fig. 7. Comparison of distribution of impact ionization generation rate at the breakdown for 4H-SiC p-i-n diode with: a) SZ-JTE and b) TZ-JTE for JTE dose 1.2×10^{17} cm^{-3}

ratios for $L_{JTE1}:L_{JTE2} = 1:1$ (Fig. 6b). With the increase of the $p_{JTE1}:p_{JTE2}$ ratio, the value of the dose for which the sudden drop in the breakdown voltage occurs is increased. For the $p_{JTE1}:p_{JTE2}$ ratio $= 1.5:1$ this dose value is about 1.66×10^{17} cm^{-3} for $p_{JTE1}:p_{JTE2} = 1.75:1 - 1.9\times10^{17}$ cm^{-3}, and for $p_{JTE1}:p_{JTE2} = 2:1$ it is about 2.24×10^{17} cm^{-3}, respectively. It is also worth noting that in the JTE dose range from the dose for maximum breakdown voltage and the dose at which the breakdown voltage falls suddenly, the breakdown voltage value reach a certain local minimum, the value of which decreases with the $p_{JTE1}:p_{JTE2}$ ratio. For $p_{JTE1}:p_{JTE2} = 1.5:1$ the value of this voltage is 2100 V, for $p_{JTE1}:p_{JTE2} = 1.75:1$, is about 1945 V, and for $p_{JTE1}:p_{JTE2} = 2:1$ it is about 1875V, respectively. Figure 8 shows the distribution of impact ionization generation rate at the breakdown for 4H-SiC p-i-n diode with TZ-JTE with JTE dose of 2.2×10^{17} cm^{-3} and different $p_{JTE1}:p_{JTE2}$ ratio 1.5 : 1, 1.75 : 1 and 2 : 1 and $L_{JTE1}:L_{JTE2} = 1:1$. Distribution of carrier generation in the case of TZ-JTE diode with a $p_{JTE1}:p_{JTE2}$ ratio of 2 : 1 is the most uniform, especially in the area under the contact of the anode and at the inner edge of JTE. This is correlated with the breakdown voltage values presented in Fig. 6b.

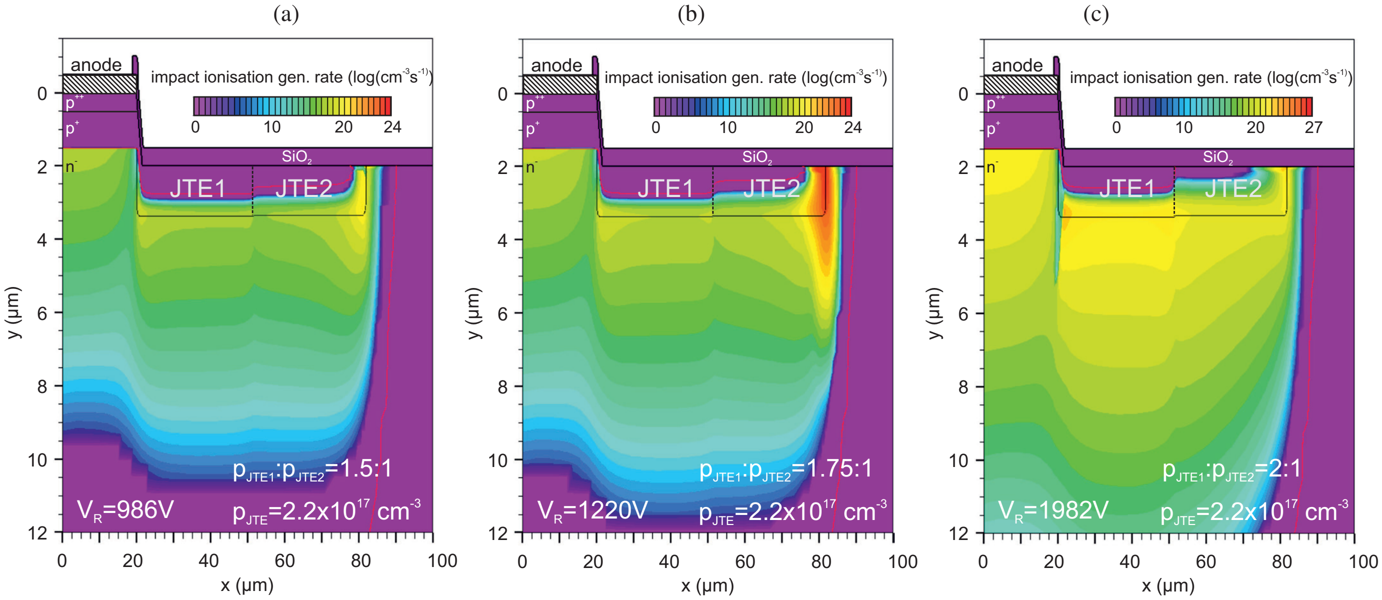

Fig. 8. Distribution of impact ionization generation rate at the breakdown for 4H-SiC p-i-n diode with TZ-JTE with JTE dose 2.2×10^{17} cm^{-3} and different $p_{JTE1}:p_{JTE2}$ ratio: a) 1.5 : 1; b) 1.75 : 1; c) 2 : 1 for $L_{JTE1}:L_{JTE2} = 1:1$

3.3. Space-modulated junction termination extension (SM-JTE). For further improvement the tolerance of breakdown voltage value on the JTE dose, a space-modulated JTE structure consisting of rings outside each of the JTE areas in the TZ-JTE structure was introduced, with a more smooth change in the space charge in the JTE structure [9–11]. It was assumed that the number of rings is 1, 2 or 3 (ring width 2 μm, distance between rings 2 μm), the total length of the JTE area was 60 μm for the ratio $L_{JTE1} : L_{JTE2} = 1 : 1$, with a total dose from 4×10^{16} cm^{-3} to 4×10^{17} cm^{-3}.

Figure 9 shows the dependence of the breakdown voltage of 4H-SiC p-i-n diode with SZ-JTE and SM-JTE for 1, 2, and 3 rings as a function of JTE total dose. For SM-JTE, the widest range of breakdown voltage modulation and low sensitivity to the change of the dose in the JTE area were obtained. With the increase in the number of rings in the SM-JTE structure, the range of the dose in which a dose change causes a small change in the breakdown voltage was increased. Moreover, after reaching a certain value of the dose, there is no sudden drop in breakdown voltage in the opposite to SZ-JTE and TZ-JTE structures. The value of the dose for which breakdown voltage is below the assumed value of 1700 V is 2.5×10^{17} cm^{-3}, 2.8×10^{17} cm^{-3} and 3.3×10^{17} cm^{-3} for SM-JTE with 1, 2 and 3 rings, respectively. The optimal value of the dose in JTE area, for which breakdown voltage reaches the maximum, was 1.2×10^{17} cm^{-3} regardless of the number of the rings. There was also a slight increase in the maximum breakdown voltage (2316 V) as compared to 2293 V for a SZ-JTE and TZ-JTE structure.

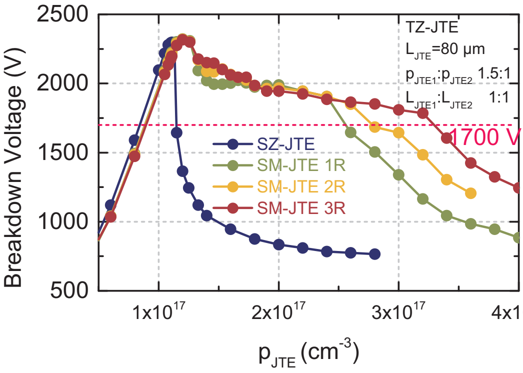

Fig. 9. Breakdown voltage of 4H-SiC p-i-n diode with SM-JTE as a function of JTE dose for different rings numbers

The observed effects are related to a better control of electric field distribution at the breakdown in the diode with SM-JTE in comparison to the diode with SZ-JTE and TZ-JTE structures. Figure 10 shows the distribution of impact ionization generation rate at the breakdown for 4H-SiC p-i-n diode with SZ-JTE and SM-JTE with three rings for JTE dose of 2×10^{17} cm^{-3}. In the case of the SM-JTE structure, the breakdown occurs in the JTE1 area, at the outer edge of the JTE1 with more uniform distribution of impact ionization generation rate within this area. In comparison, in case of SZ-JTE structure the breakdown occurs at the outer edge of the JTE area.

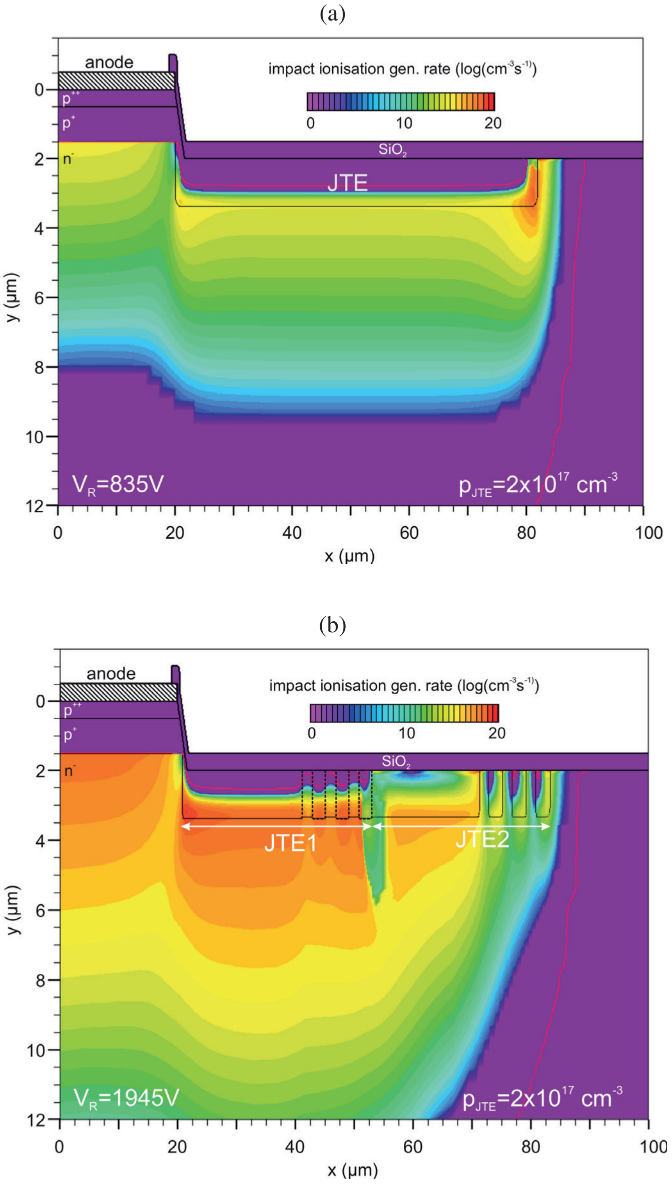

Fig. 10. Comparison of distribution of impact ionization generation rate at breakdown for 4H-SiC p-i-n diode with: a) SZ-JTE and b) SM-JTE with three rings for JTE dose 2×10^{17} cm^{-3}

Simulations were also carried out to investigate how surface charge density at the interface of the JTE area and SiO_2 layer Q_{it} ranging from $+1\times10^{11}$ cm^{-2} to $+1\times10^{13}$ cm^{-2} on the breakdown voltage of the p-i-n diode with SM-JTE with three rings and a total JTE dose of 1.2×10^{17} cm^{-3} and 1.6×10^{17} cm^{-3}, i.e. for an optimal dose and a dose slightly more than optimal one. Figure 11 shows the impact of the Q_{it} affects breakdown voltage of the SM-JTE diode for $p_{JTE} = 1.2\times10^{17}$ cm^{-3} and $p_{JTE} = 1.6\times10^{17}$ cm^{-3} compared to SZ-JTE for $p_{JTE} = 1.1\times10^{17}$ cm^{-3}. In the case of the SM-JTE structure with three rings, for $p_{JTE} = 1.2\times10^{17}$ cm^{-3} (i.e. the dose at which the breakdown voltage reaches the maximum), the breakdown voltage dependence on the Q_{it} value is similar to that of a SZ-JTE structure. Different behavior is observed in the case of the SM-JTE diode with three rings for a dose $p_{JTE} = 1.6\times10^{17}$ cm^{-3}. The shift of the dependence of the breakdown voltage on the

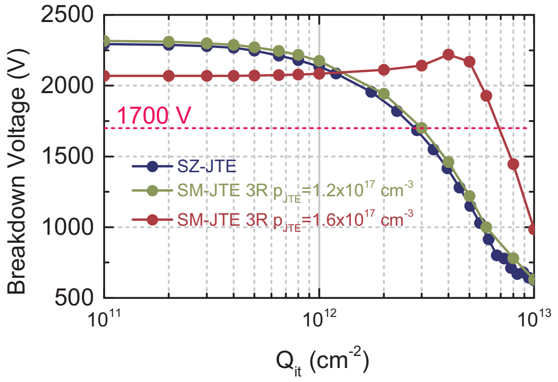

Fig. 11. The dependence of the breakdown voltage of 4H-SiC p-i-n diode with SZ-JTE for $p_{JTE} = 1.1\times10^{17}$ cm^{-3} and for a diode with SM-JTE with three rings for $p_{JTE} = 1.2\times10^{17}$ cm^{-3} and $p_{JTE} = 1.6\times10^{17}$ cm^{-3} as a function of Q_{it} values

JTE dose as a result of the Q_{it} does not reduce breakdown voltage, but even increases its value, reaching a maximum of 2220 V for $Q_{it} = +4\times10^{12}$ cm^{-2}. This is related to the much higher breakdown voltage tolerance to the JTE dose value for the SM-JTE structure as compared to the SZ-JTE structure. As can be seen in Fig. 4a, the existence of interface charge shifts the breakdown voltage $-p_{JTE}$ curves towards higher p_{JTE} values. This can be understood as lowering the effective dose of JTE with increasing Q_{it} values. In the case of SM-JTE with $p_{JTE} = 1.6\times10^{17}$ cm^{-3} the increase of Q_{it} results in much stable behavior of breakdown voltage with respect to Q_{it} as with decreasing of effective p_{JTE} dose from nominal value, the breakdown voltage is increasing (as can be seen in Fig. 9) reaching maximum value and then drops for the effective p_{JTE} dose lower then optimal dose in JTE area (1.2×10^{17} cm^{-3} in this case), for which the breakdown voltage reaches the maximum. In the case of SM-JTE with $p_{JTE} = 1.2\times10^{17}$ cm^{-3}, increasing of Q_{it} and at the same time lowering of effective p_{JTE} dose results in decreasing of breakdown voltage in the same manner as for SZ-JTE diode, which is related to the fact that for the p_{JTE} dose lower than optimal one, the slope of relationship between breakdown voltage and p_{JTE} dose for SM-JTE is the same as in the case of the SZ-JTE structure (see Fig. 9). A similar reduction of sensitivity to Q_{it} is also expected for TZ-JTE structures for the nominal p_{JTE} values higher than optimal p_{JTE} dose.

In this work, the influence of statistical dispersion of active layer parameters, i.e. doping ($N_{D,epi}$) and drift layer thickness (t_{epi}), on breakdown voltage/efficiency of JTE structure was also examined. During the simulation for a fixed value of $N_{D,epi} = 7.2\times10^{15}$ cm^{-3}, t_{epi} values change in the range of 13±1.3 μm, thus assuming the drift layer thickness statistical variation no greater than 10%. Then, for $t_{epi} = 13$ μm, $N_{D,epi}$ values were changed $N_{D,epi} = (7.2\pm1.8)\times10^{15}$ cm^{-3}, thus assuming statistical variation of drift layer doping not higher than 25%. The SZ-JTE structure with optimal dose $p_{JTE} = 1.1\times10^{17}$ cm^{-3} and SM-JTE structure with three rings and a total dose of 1.2×10^{17} cm^{-3} and 1.6×10^{17} cm^{-3}, i.e. for an optimal dose and higher than optimal dose, were compared.

Figure 12 shows the dependence of the breakdown voltage of the 4H-SiC p-i-n diode with SZ-JTE and SM-JTE, the drift layer thickness and doping level. As the thickness of the drift layer increases, the breakdown voltage increases monotonically, and the relationship is approximately linear, both for diode with the SZ-JTE and with SM-JTE, regardless of the p_{JTE} values. For the variation of the drift layer thickness ±10%, the change of breakdown voltage is ±100 V. An important difference can be seen in the dependence of the breakdown voltage on the drift layer doping level. According to the predictions for the ideal diode structure, the breakdown voltage decreases linearly with the level of drift doping [8]. A similar relationship was observed for diode with SM-JTE regardless of the p_{JTE} value. For the SM-JTE structures, for the statistical dispersion of drift layer doping of ±25%, a change in the breakdown voltage of about ± 100V was observed. In comparison to SM-JTE for the SZ-JTE structure, a sudden drop in the breakdown voltage to 1975V was observed for $N_{D,epi} = 6.2\times10^{15}$ cm^{-3}.

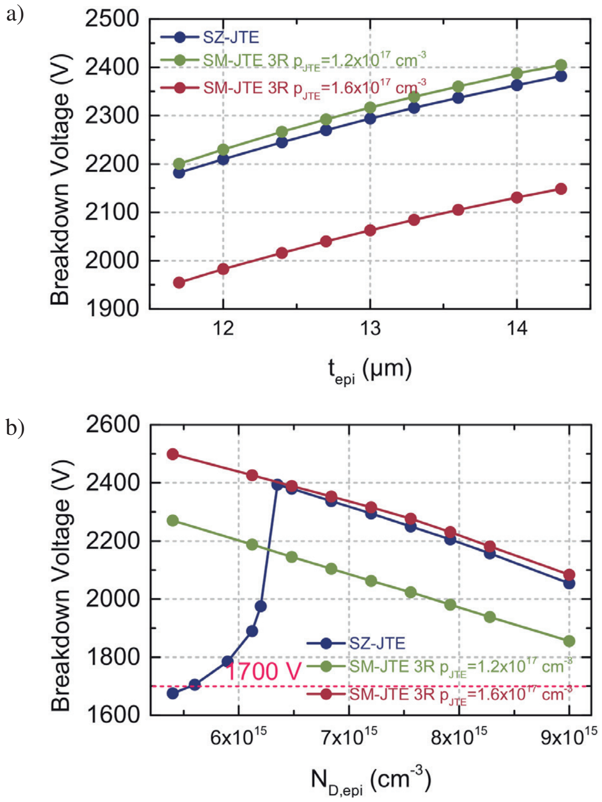

Fig. 12. The dependence of the breakdown voltage of 4H-SiC p-i-n diode with SZ-JTE for $p_{JTE} = 1.1\times10^{17}$ cm^{-3} and for a diode with SM-JTE with three rings for $p_{JTE} = 1.2\times10^{17}$ cm^{-3} and $p_{JTE} = 1.6\times10^{17}$ cm^{-3} as a function of a) drift layer thickness, b) drift layer doping density

According to Fig. 13, showing the distribution of impact ionization generation rate at the breakdown for $N_{D,epi} = 6.2\times10^{17}$ cm^{-3} and $N_{D,epi} = 6.35\times10^{17}$ cm^{-3}, in the case of doping below 6.35×10^{17} cm^{-3} a decrease of the effectiveness of the SZ-JTE area is observed, and the breakdown occurs at the outer edge of the JTE area, similarly as in the case of SZ-JTE diodes for p_{JTE} greater than optimal one (Fig. 3c).

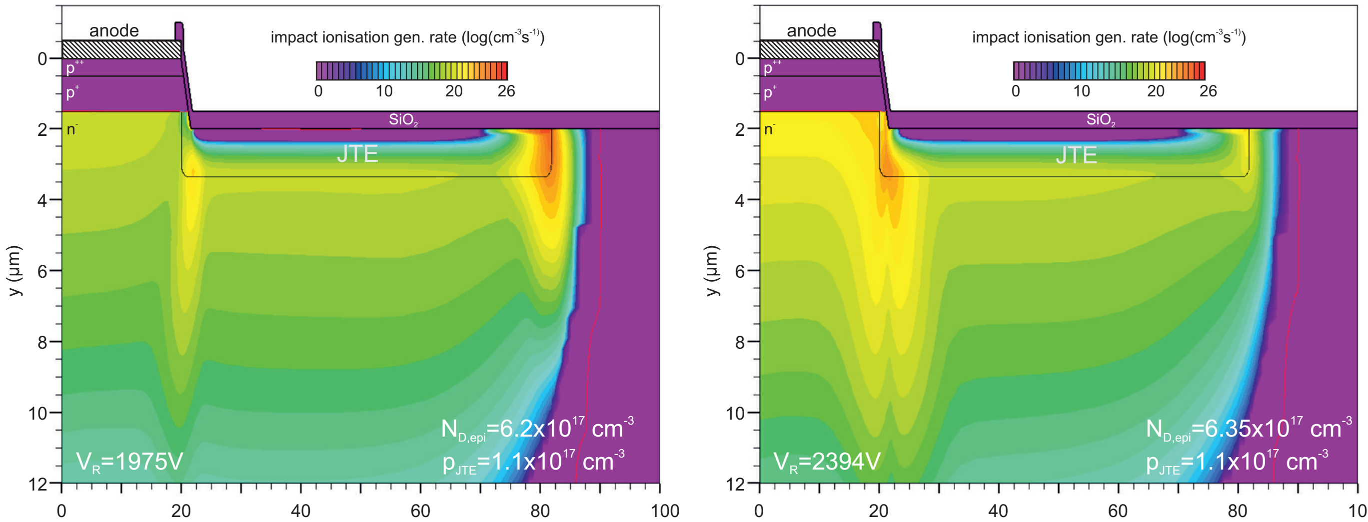

Fig. 13. Comparison of distribution of impact ionization generation rate at the breakdown for 4H-SiC p-i-n diode with SZ-JTE for JTE dose 1.1×10^{17} cm^{-3} and drift layer doping: a) $N_{D,epi} = 6.2\times10^{17}$ cm^{-3} and b) $N_{D,epi} = 6.35\times10^{17}$ cm^{-3}

4. Conclusions

In this work, in order to obtain over 1.7 kV breakdown voltage of silicon carbide p-i-n diode, three designs have been investigated: single-zone (SZ-JTE), two-zone (TZ-JTE) and space-modulated JTE (SM-JTE) structures. The influence of the length, level of p-type doping in the JTE area, as well as the charge on the surface between the p-type area and the passivation layer and statistical variation of region parameters (thickness and doping level) on the breakdown voltage of p-i-n diode was examined. The comparison of designed JTE structures for 1.7 kV 4H-SiC p-i-n diode is presented in Table 1.

The obtained results showed that the values of breakdown voltage for a diode with a single zone JTE are very sensitive due to both the level of doping and the charge accumulated on the dielectric/semiconductor interface. The use of double zone or space modulated JTE allows to obtain breakdown voltage above 1.7 kV for a much wider range of p-type doping parameters. This is very important due to lower requirements for the fabrication of JTE by means of aluminium ion implantation and high temperature dopant activation. Thanks to the use of the space modulated JTE with three outer rings, a wide doping range that allows obtaining a breakdown voltage diode above 1.7 kV was obtained, varying from 8.9×10^{16} cm^{-3} to 3.3×10^{17} cm^{-3}, compared to the range of doping from 8.43×10^{16} cm^{-3} up to 1.15×10^{17} cm^{-3} for a single zone JTE design. Optimized JTE design with three outer rings allows to reduce the influence of interface charge as well as statistical variation of active layers parameters on the breakdown voltage of 1.7 kV 4H-SiC p-i-n diodes.

Table 1
Comparison of designed JTE structures for 1.7 kV 4H-SiC p-i-n diode

JTE structure	design parameters	max. V_{BR}	dose range (for $V_{BR} > 1700$ V)	reduction of sensitivity to Q_{it}
SZ-JTE	$L_{JTE} = 60$ µm	2293 V	8.43×10^{16} cm^{-3}–1.15×10^{17} cm^{-3}	no
TZ-JTE	$L_{JTE} = 60$ µm, $L_{JTE1} : L_{JTE2} = 1 : 1$			
	$p_{JTE1} : p_{JTE2} = \mathbf{1.5 : 1}$	2293 V	8.45×10^{16} cm^{-3}–1.7×10^{17} cm^{-3}	yes
	$p_{JTE1} : p_{JTE2} = \mathbf{1.75 : 1}$	2293 V	8.45×10^{16} cm^{-3}–2×10^{17} cm^{-3}	yes
	$p_{JTE1} : p_{JTE2} = \mathbf{2{:}1}$	2293 V	8.45×10^{16} cm^{-3}–2.28×10^{17} cm^{-3}	yes
SM-JTE	$L_{JTE} = 60$ µm, $L_{JTE1} : L_{JTE2} = \mathbf{1 : 1}$			
	$p_{JTE1} : p_{JTE2} = 1.5 : 1$, $r_{width} = 2$ µm, $r_{space} = 2$ µm			
	1 ring	2316 V	8.9×10^{16} cm^{-3}–2.55×10^{17} cm^{-3}	yes
	2 rings	2316 V	8.9×10^{16} cm^{-3}–2.8×10^{17} cm^{-3}	yes
	3 rings	2316 V	8.9×10^{16} cm^{-3}–3.3×10^{17} cm^{-3}	yes

Acknowledgements. This work was supported by The Polish National Centre for Research and Development under Agreement nr TECHMATSTRATEG1/346922/4/NCBR/2017 for project "Technologies of semiconductor materials for high power and high frequency electronics".

REFERENCES

[1] R.R. Potera and T.J. Han, "Silicon Carbide Diodes in Power-Factor Correction Circuits: Device and Circuit Design Aspects", *IEEE Power Electron. Mag.* 6(1), 34–39 (2019).

[2] M. Maciążek and M. Pasko, "Optimum allocation of active power filters in large supply systems", *Bull. Pol. Ac.: Tech.* 64(1), 37–44 (2016).

[3] W. Janke, A. Hapka, and M. Oleksy, "DC characteristics of the SiC Schottky diodes", *Bull. Pol. Ac.: Tech.*, 59(2) 183–188 (2011).

[4] J. Woźny, A. Kovalchuk, Z, Lisik, J. Podgórski, P. Bugalski, A. Kubiak and Ł. Ruta, "DFT simulation of stacking faults defects in 4H-SiC", *2018 XIV-th International Conference on Perspective Technologies and Methods in MEMS Design (MEMSTECH), Lwów*, 65–68 (2018).

[5] H.W. Kim, W. Bahng, G.H. Song, S.C. Kim, N.K. Kim, and E.D. Kim, "Edge Termination Technique for SiC Power Devices", *Mater. Sci. Forum* 457–460, 1241–1244 (2004).

[6] V.A.K. Temple and W. Tantraporn, "Junction termination extension for near-ideal breakdown voltage in p-n junctions", *IEEE Trans. Electron Devices*, 33(10), 1601–1608 (1986).

[7] A. Mahajan and B.J. Skromme, "Design and optimization of junction termination extension (JTE) for 4H–SiC high voltage Schottky diodes", *Solid-State Electronics* 49(6), 945–955 (2005).

[8] T. Hiyoshi, T. Hori, J. Suda, and T. Kimoto, "Simulation and Experimental Study on the Junction Termination Structure for High-Voltage 4H-SiC PiN Diodes", *IEEE Trans. Electron Devices* 55(8), 1841–1846 (2008).

[9] B.J. Baliga, *Fundamentals of Power Semiconductor Devices*, Springer International Publishing AG, 2019.

[10] Y. Huang, Y. Wang, X. Kuang, W. Wang, J. Tang, and Y. Sun, "Step-Double-Zone-JTE for SiC Devices with Increased Tolerance to JTE Dose and Surface Charges", *Micromachines* 9(12), 610 (2018).

[11] G. Feng, J. Suda, and T. Kimoto, "Space-Modulated Junction Termination Extension for Ultrahigh-Voltage p-i-n Diodes in 4H-SiC", *IEEE Trans. Electron Devices* 59(2), 414–418 (2012).

[12] H. Niwa, J. Suda, and T. Kimoto, "21.7 kV 4H-SiC PiN Diode with a Space-Modulated Junction Termination Extension", *Appl. Phys. Express* 5(6), 064001 (2012).

[13] K. Nakayama et al., "27.5 kV 4H-SiC PiN diode with space-modulated JTE and carrier injection control", *2018 IEEE 30th International Symposium on Power Semiconductor Devices and ICs (ISPSD)*, 395–398 (2018).

[14] V.K. Khanna, *Insulated Gate Bipolar Transistor IGBT Theory and Design*, IEEE Press, New Jersey, 2003.

[15] Silvaco ATLAS User's Manual (2019).

[16] T. Hatakeyama, T. Watanabe, T. Shinohe, K. Kojima, K. Arai and N. Sano, "Impact ionization coefficients of 4H silicon carbide", *Appl. Phys. Lett.* 85(8), 1380 (2004).

[17] T. Hatakeyama, "Measurements of impact ionization coefficients of electrons and holes in 4H-SiC and their application to device simulation", *Phys. Status Solidi (a)*, 206(10), 2284–2294 (2009).

[18] R. Ghandi et al., "Surface-Passivation Effects on the Performance of 4H-SiC BJTs", *IEEE Trans. Electron Devices* 58(1), 259–265 (2011).

[19] A. Taube, M. Guziewicz, K. Kosiel, K. Gołaszewska-Malec, K. Król, R. Kruszka, E. Kamińska, and A. Piotrowska, "Characterization of Al_2O_3/4H-SiC and Al_2O_3/SiO_2/4H-SiC MOS structures", *Bull. Pol. Ac.: Tech.* 64(3), 547–551 (2016).

[20] K.B. Król, *Dielectrics produced by thermal methods in silicon carbide for MOS semiconductor devices*, PhD thesis (in Polish), Warsaw University of Technology, Faculty of Electronics and Information Technology, Warsaw (2015).

[21] K. Król, M. Sochacki, W. Strupinski, K. Racka, M. Guziewicz, P. Konarski, M. Misnik, and J. Szmidt, "Chlorine-enhanced thermal oxides growth and significant trap density reduction at SiO_2/SiC interface by incorporation of phosphorus", *Thin Solid Films*, 591(A), 86–89, (2015).